



HAL
open science

Effect of heterostructure design on current-voltage characteristics in $\text{Al}_x\text{Ga}_{1-x}\text{N}/\text{GaN}$ double-barriers resonant tunneling diode

Mohamed Boucherit, Ali Soltani, Michel Rousseau, J.L. Farvacque,
Jean-Claude de Jaeger

► **To cite this version:**

Mohamed Boucherit, Ali Soltani, Michel Rousseau, J.L. Farvacque, Jean-Claude de Jaeger. Effect of heterostructure design on current-voltage characteristics in $\text{Al}_x\text{Ga}_{1-x}\text{N}/\text{GaN}$ double-barriers resonant tunneling diode. *Journal of Applied Physics*, 2012, 112 (11), pp.114305. 10.1063/1.4767382. hal-00787875

HAL Id: hal-00787875

<https://hal.science/hal-00787875>

Submitted on 25 May 2022

HAL is a multi-disciplinary open access archive for the deposit and dissemination of scientific research documents, whether they are published or not. The documents may come from teaching and research institutions in France or abroad, or from public or private research centers.

L'archive ouverte pluridisciplinaire **HAL**, est destinée au dépôt et à la diffusion de documents scientifiques de niveau recherche, publiés ou non, émanant des établissements d'enseignement et de recherche français ou étrangers, des laboratoires publics ou privés.

Effect of heterostructure design on current-voltage characteristics in $\text{Al}_x\text{Ga}_{1-x}\text{N}/\text{GaN}$ double-barriers resonant tunneling diode

Cite as: J. Appl. Phys. **112**, 114305 (2012); <https://doi.org/10.1063/1.4767382>

Submitted: 15 August 2012 • Accepted: 26 October 2012 • Published Online: 03 December 2012

M. Boucherit, A. Soltani, M. Rousseau, et al.



View Online



Export Citation



CrossMark

ARTICLES YOU MAY BE INTERESTED IN

[Investigation of the negative differential resistance reproducibility in AlN/GaN double-barrier resonant tunnelling diodes](#)

Applied Physics Letters **99**, 182109 (2011); <https://doi.org/10.1063/1.3659468>

[Asymmetric quantum-well structures for AlGaIn/GaN/AlGaIn resonant tunneling diodes](#)

Journal of Applied Physics **119**, 164501 (2016); <https://doi.org/10.1063/1.4948331>

[Quantitative analysis of the trapping effect on terahertz AlGaIn/GaN resonant tunneling diode](#)

Applied Physics Letters **99**, 153501 (2011); <https://doi.org/10.1063/1.3650253>

Lock-in Amplifiers
up to 600 MHz



Zurich
Instruments



Effect of heterostructure design on current-voltage characteristics in $\text{Al}_x\text{Ga}_{1-x}\text{N}/\text{GaN}$ double-barriers resonant tunneling diode

M. Boucherit,¹ A. Soltani,¹ M. Rousseau,¹ J.-L. Farvacque,²
and J.-C. DeJaeger¹

¹IEMN/UMR CNRS 8520, Université Lille1, PRES Université Lille Nord de France, Cité scientifique,
Avenue Poincaré, 59652 Villeneuve d'Ascq, France

²UMET/UMR CNRS 8207, Université Lille1, PRES Université Lille Nord de France, Cité scientifique, Bât/C6,
59652 Villeneuve d'Ascq, France

(Received 15 August 2012; accepted 26 October 2012; published online 3 December 2012)

Ballistic transport in double-barriers resonant tunneling diodes based on GaN is investigated in this work using the non-equilibrium Green's functions formalism. The electron density of states, the electrons concentration, and the current-voltage characteristics are calculated taking into account the internal electric field induced in the $\text{Al}_x\text{Ga}_{1-x}\text{N}/\text{GaN}$ heterostructures. The effect of the geometrical parameters on the evolution of the current resonances characteristics was analyzed qualitatively by varying GaN quantum well width, thicknesses and height of the $\text{Al}_x\text{Ga}_{1-x}\text{N}$ barriers. © 2012 American Institute of Physics. [<http://dx.doi.org/10.1063/1.4767382>]

I. INTRODUCTION

Thanks to their strong negative differential resistance (NDR), the double-barriers resonant tunneling diodes (RTDs) have attracted great interest for use as compact and coherent terahertz (THz) sources operating at room temperature.¹ Due to their large conduction band offset between AlN/GaN heterostructure (1.75 eV),² the RTDs based on GaN should permit to obtain higher voltage and power operation in comparison with conventional III-V semiconductors. However, the $\text{Al}_x\text{Ga}_{1-x}\text{N}/\text{GaN}$ heterostructures possess strong polarization charges at the heterointerfaces that make difficult to model the vertical electronic transport in RTDs devices. Until now, only a few theoretical studies have been performed on $\text{Al}_x\text{Ga}_{1-x}\text{N}/\text{GaN}$ RTDs.³⁻⁵

In this work, we have chosen to use the non-equilibrium Green's functions (NEGF) approach to provide qualitative comprehension of the ballistic transport in the III-nitride RTDs. Indeed, the NEGF formalism is a pertinent technique to describe quantum devices, especially the tunneling current. From this approach, a computer code was developed to calculate electrical properties of $\text{Al}_x\text{Ga}_{1-x}\text{N}/\text{GaN}$ RTDs. The NEGF method is also well suited treating semi-infinite contacts attached to an intrinsic device. The open boundary conditions are treated through the self-energies functions Σ^R and Σ^A . This method is well adapted for our case whereas the transfer-matrix method is generally not suitable because it deals with isolated systems.⁵ However, our interest is often in open systems with strong coupling to the contacts.

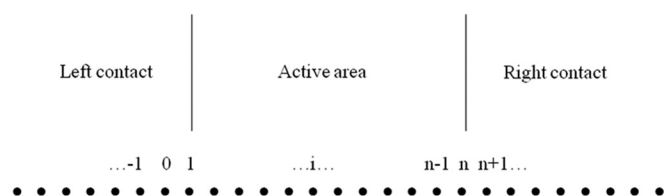
The paper is organized as follows: Section II describes the simulation model, Sec. II A deals with self-energy boundary conditions, Sec. II B summarizes equations to be used in NEGF formalism, Sec. II C explains the procedure to calculate the potential profile self-consistently; and Sec. III describes the simulation results, Sec. III A analyses the effect of GaN quantum well (QW) width, Sec. III B investigates the effect of $\text{Al}_x\text{Ga}_{1-x}\text{N}$ barriers' thicknesses, and Sec. III C studies the effect of $\text{Al}_x\text{Ga}_{1-x}\text{N}$ barriers' height.

II. SIMULATION MODEL

Since electrostatic potential varies only along the growth direction (1000) (axis z), the RTD is considered as one dimensional device (translationally invariant in the (x,y) plane) consisting of an active area connected to two semi-infinite contacts. Also, as the RTDs operation involves only the electrons in a parabolic conduction band, the effective mass approximation is assumed to be valuable at this scale. This assumption becomes progressively poorer with the decrease in structure thickness. However, we note that the effective mass approximation still is a reasonable approximation for our structure. Thus, to obtain the electronic wave functions in the device, the Schrodinger's equation is solved in the active area and contacts

$$-\frac{\hbar^2}{2m^*} \frac{d^2\psi}{dz^2} + U(z)\psi = E(z)\psi,$$

where, E is the energy, m^* is the effective mass, and $U(z) = V_{BC} + V_{piez} + V_{appl} + U_H$ is the potential profile that includes V_{BC} the conduction band profile, V_{piez} the piezoelectric field, V_{appl} the applied bias voltage, and U_H the self-consistent space charge within the Hartree approximation



By setting 1D spatial grid points with uniform spacing lattice constant a , the finite difference method is used to write the Schrodinger equations in the active area and semi-infinite contacts

It might appear that the self-energy method used by NEGF formalism is just another method for handling boundary effects, as the periodic boundary conditions used by the transfer-matrix method, where $\psi_{L,0} = \psi_n$ and $\psi_{R,n+1} = \psi_1$. However, the full power of the self-energy method becomes apparent when the device is under bias, a problem that cannot be handled with periodic boundary conditions.⁷ Indeed, given the nanoscale of the active area, the imaginary parts $\Gamma = i[\Sigma^R - \Sigma^A]$ introduced by the self-energies functions change non-negligibly the available local density of states in the active area (see Sec. II B, Eq. (5)). Here, $\Sigma^A = \Sigma^{R-1}$ is the advanced self-energies.

B. NEGF equations

Due to its nanoscale size, the active area is assumed to be a ballistic region connected to two semi-infinite contacts. Thereby, the inelastic scattering processes inside the device is neglected. In the NEGF formalism, the retarded Green's function G^R is the key equation that contains information on the distribution of available states: $G^R = \sum_{\alpha} \frac{|\psi\rangle\langle\psi|}{E - E_{\alpha}}$,⁶ where, $|\psi\rangle$ and E_{α} refer to eigenstates and eigenvalues of the Hamiltonian, respectively.

In the NEGF formalism, the spectral function A represents the available local density of states in the RTD

$$A = G^R \Gamma G^A, \quad (5)$$

where, $G^A = G^{R-1}$ is the advanced Green's function. Eq. (5) should be multiplied by 2 for spin degeneracy. The diagonal elements of A are the quantity of interest which yields directly to the local density of states

$$LDOS(r, E) = \frac{1}{2\pi} A(r, E).$$

Thus, the local electron density $n(z)$ in the device is given by

$$n(r) = 1/2\pi \int f_L(E) A_L(r, E) + f_R(E) A_R(r, E) dE,$$

where $f_L(E)$ and $f_R(E)$ are the Fermi functions of the left and right contacts, respectively.

At the ballistic limit, the current can be expressed in terms of the distribution functions in the contacts and the transmission function: $I = 2e/h \int [f_L(E) - f_R(E)] \text{Tr}(\Gamma_L G^R \Gamma_R G^A) dE$.

C. Poisson equation

Our self-consistent simulation approach feedbacks the electron density $n(r)$ into the Poisson equation: $d^2 U_H / dr^2 = q^2 / \epsilon [N_D^+ - n(r)]$. The latter is used to compute U_H the self-consistent space charge within the Hartree approximation. The process is repeated until the difference between the old and new potentials becomes less than the desired tolerance. For the first iteration, the initial electron density $n_{\text{init}}(r)$ is obtained by setting $U_H^{\text{init}} = 0$ into the potential profile $U_{\text{init}}(r)$ of the Hamiltonian matrix.

III. SIMULATION RESULTS

In order to study the tunneling current evolution versus RTD design, thicknesses of the i-GaN spacers were fixed at

4 mono-layers (MLs) (1 nm). The positive voltage corresponds to conditions under which the top electrode is positively biased and the buffer is negatively biased. The internal fields produced by spontaneous and piezoelectric polarizations are taken into account in the context of the macroscopic approach. At the AlN/GaN heterointerface, we have assumed alternating polarization charge densities of $\sigma = 6.5 \times 10^{13} \text{ cm}^{-2}$, according to Ga face polarity of the structure in the growth direction.⁴

A. Effect of GaN quantum well width

In the following, the current-voltage characteristics are discussed in detail with respect to the GaN QW width. All combinations between 4 and 8 MLs for the GaN QW thicknesses are simulated by fixing the percentage of aluminium $\text{Al}_x\text{Ga}_{1-x}\text{N}$ barriers to $x = 1.0$ and maintaining the AlN barriers' thicknesses at 4 MLs. A self-consistent calculation of the conduction band profile was performed in Figure 1. The latter simulation has shown that the spontaneous and piezoelectric polarizations induce a strong asymmetry in the conduction band profile. Thus, the internal electric fields associated with these polarizations lead to the formation of a two dimensional electron gas and depletion region near the AlN/GaN interfaces, in the side of the cathode and anode, respectively.

The resulting current-voltage behavior leads to a significant current peak in only one direction voltage (Fig. 2). At positive voltages, the directions of the external and internal fields are opposite. These result in a large charge accumulated in the quantum well (Fig. 3). At negative voltages, the directions of the external and internal fields in the QW are the same. Thus, the value of the charge in the QW is smaller, and therefore, the current peak intensities are smaller.⁸ The electron density of states for these AlN/GaN investigated structures has also been computed (Fig. 4). Thus, we have attributed the first series of resonant peaks (S_1) to the resonant tunnelling through the fundamental quasi-bound states in the QW and the second series (S_2) to the tunnelling through the excited quasi-bound states near the double-barriers edges (Fig. 2).⁵

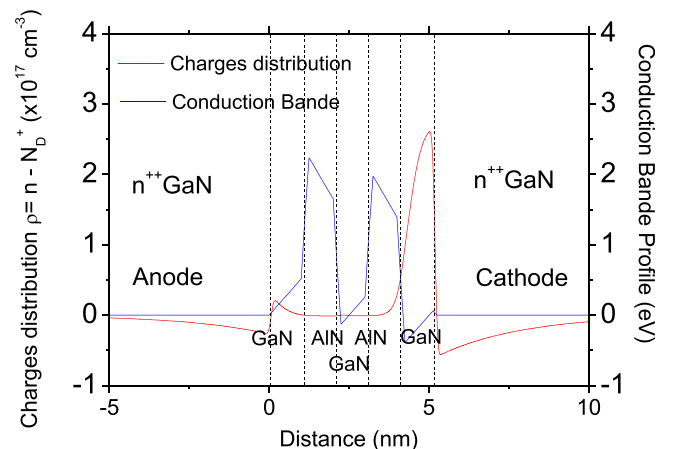


FIG. 1. Conduction band profile and charges distribution at 0 V corresponding to the (4/4) MLs structure.

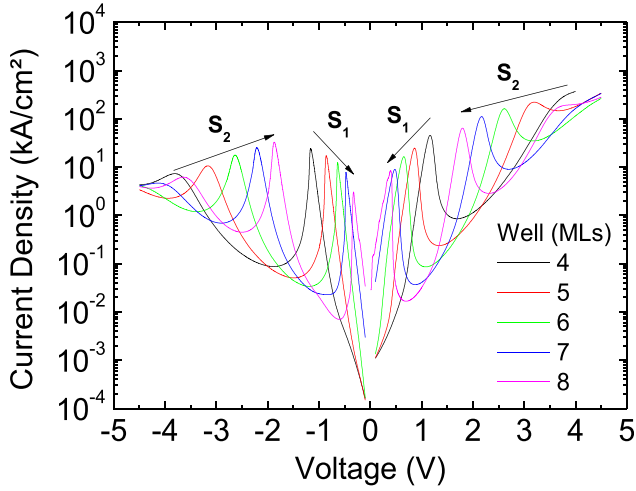
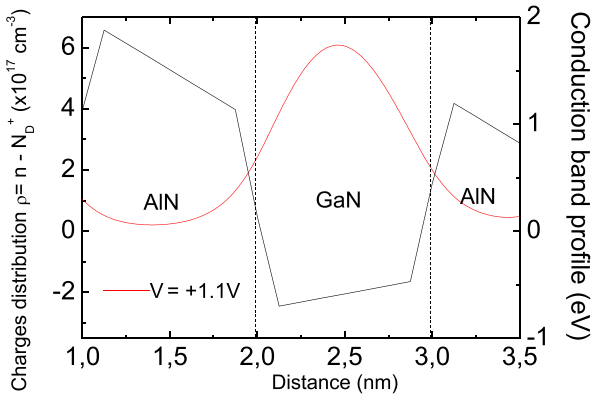


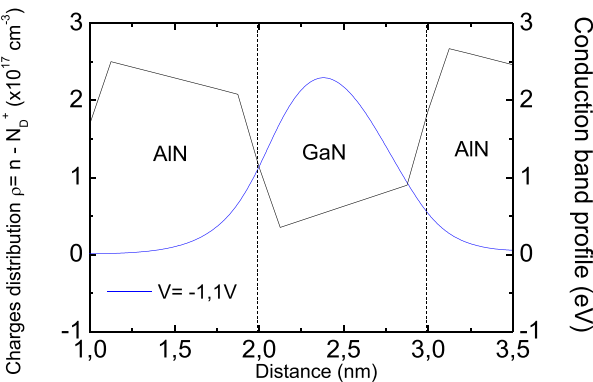
FIG. 2. Current density versus voltage for different thicknesses of GaN well.

B. Effect of Al_xGa_{1-x}N barriers' thicknesses

To emphasize the importance of triangular barriers band bending, different Al_xGa_{1-x}N barriers' thicknesses varying from 4 to 8 MLs are simulated by maintaining this time the GaN well thickness at 4 MLs and fixing the percentage of aluminium to $x = 1.0$. The results of our computations show that by increasing the AlN barriers' thicknesses, the current



(a)



(b)

FIG. 3. Charges distribution in the GaN well of the (4/4/4) MLs structure (a) at $V = +1.1$ V and (b) $V = -1.1$ V.

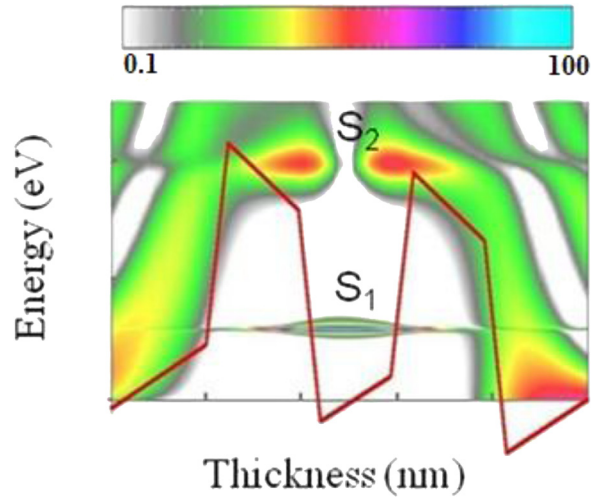


FIG. 4. Conduction band profile corresponding to the (4/4/4) MLs structure.

valley decreases much faster than the current peak (Fig. 5). Thereby, the peak-to-valley current ratio increases. Furthermore, the current peaks are less pronounced. Indeed, the polarization discontinuities between AlN and GaN increase with the barriers' thicknesses. The latter involves much larger depletion region that leads to a reduction in the resonant peak intensities. Moreover, the voltage valley positions change significantly due to the decrease of the electrons probability transmission.

C. Effect of Al_xGa_{1-x}N barriers' height

At last, the effect of the barriers' height is studied by varying the Al composition from $x = 0.2$ to $x = 1.0$. The GaN well and the Al_xGa_{1-x}N barriers' thicknesses were fixed at 4 MLs. The results of our computations show that by increasing the Al composition, the peak-to-valley current ratio increases (Fig. 6). It is clear that the conduction band offset and the polarization discontinuity between Al_xGa_{1-x}N and GaN increase with the aluminum composition. The increase of the conduction band offset discontinuity gives

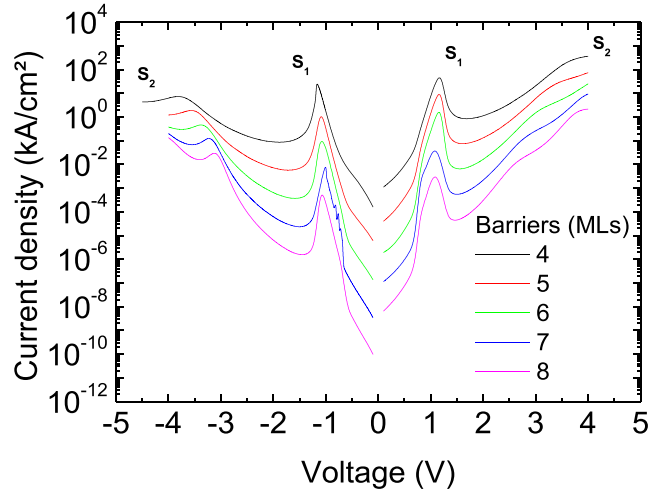


FIG. 5. Current density versus voltage for different thicknesses of AlN barriers.

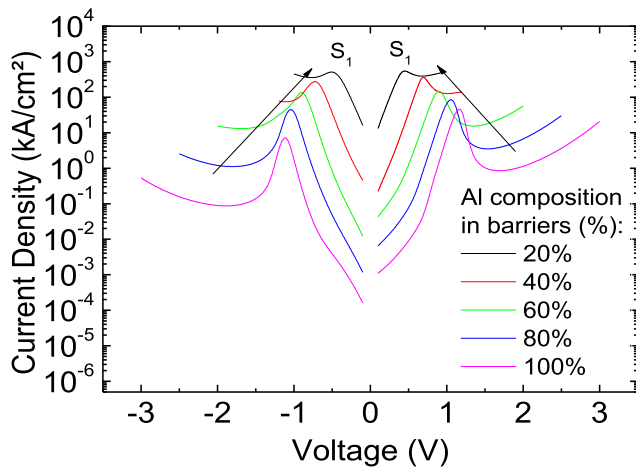


FIG. 6. Current density versus voltage for different Al contents of the $\text{Al}_x\text{Ga}_{1-x}\text{N}$ barriers corresponding to the (4/4/4) MLs structure.

rise to higher barriers that lead to a shift of the resonant peaks toward smaller voltages. Moreover, the increase of the polarization discontinuity causes a much more important internal electric field. The latter involves much larger depletion region that leads to a reduction in the resonant peak intensities.

IV. SUMMARY

In summary, we have applied the NEGF formalism to the $\text{Al}_x\text{Ga}_{1-x}\text{N}/\text{GaN}$ RTD. We have also shown that the spontaneous and piezoelectric polarizations induce a strong asymmetry in the conduction band profile that has significant effects on the current-voltage characteristics behaviour. Finally, we have discussed the tunneling resonant current evolution versus the GaN well width, thicknesses and height of $\text{Al}_x\text{Ga}_{1-x}\text{N}$ barriers.

This work was supported in part by the French Research National Agency in the frame of TRANSNIT Project No. 06-3-156347.

¹M. Asada, S. Suzuki, and N. Kishimoto, *Jpn. J. Appl. Phys., Part 1* **47**, 4375–4384 (2008).

²M. Boucherit, A. Soltani, E. Monroy, M. Rousseau, D. Deresmes, M. Berthe, C. Durand, and J.-C. De Jaeger, *Appl. Phys. Lett.* **99**, 182109 (2011).

³F. Sacconi, A. Di Carlo, and P. Lugli, *Phys. Status Solidi A* **190**, 295 (2002).

⁴K. M. Indlekofer, E. Dona, J. Malindretos, M. Bertelli, M. Kocan, A. Rizzi, and H. Luth, *Phys. Status Solidi B* **234**, 769 (2002).

⁵S. Sakr, E. Warde, M. Tcherycheva, and F. H. Julien, *J. Appl. Phys.* **109**, 23717 (2011).

⁶S. Datta, in *Proceedings of the International Electron Devices Meeting* (2002), p. 703.

⁷S. Datta, *Superlattices Microstruct.* **28**, 256 (2000).

⁸S. N. Grinyaev and A. N. Razzhvalov, *Semiconductors* **40**(6), 675 (2006).